

IR Spectrophotometric Observations of Geosynchronous Satellites

Mark A. Skinner, Tamara E. Payne

The Boeing Company

Ray W. Russell, David Gutierrez, Kirk Crawford, Daryl Kim, David K. Lynch, Dee W.

Pack, Richard J. Rudy

The Aerospace Corporation

David M. Harrington

The University of Hawaii Institute for Astronomy

ABSTRACT

We have observed several geosynchronous satellites at the Advanced Electro-Optical System (AEOS) 3.6 meter telescope, utilizing The Aerospace Corporation's Broadband Array Spectrograph System (BASS) 3-13 micron sensor, as well as other sensors. The various satellites show different trends with phase angle, which may allow satellite identification based on observables. Data were collected on several nights, on multiple satellites, and at various phase angles for each satellite. We describe our methods, data, analysis, and results.

1. INTRODUCTION

When one looks into the night sky, one sees many objects in the solar system and our galaxy (including the Milky Way from a dark site). If one looks for a while, one may often see objects move. These are sometime "shooting stars", but are more often man-made satellites in low Earth orbits. They are generally apparent as they are for the most part bright (a selection effect), and they also move rapidly with respect to the "fixed" background stars and planets. Of importance to our modern-day society is, however, the geostationary satellites that provide telecommunications, weather monitoring, and similar services. These are much harder to detect, as they are much fainter (generally $V \sim 15$), and they move only very slowly with respect to the background stars. However, as Fig. 1 shows, if observed with a sensitive telescope tracking the rate of the geo satellites, they can be readily detected.

Even though outer space is "big", the volume of space available that allows geostationary objects is small and finite. It consists of a narrow band region centered on the Earth's equator completely surrounding the Earth. The belt is loaded with high value assets from many countries (the total economic value of all the geo satellites is many trillions of dollars). Satellite Operators are allocated only a small fraction of the geo belt in which to maintain the orbit of their satellite. It is fair to say that the geo belt is crowded, especially over highly populated landmasses.

Geostationary satellites are "stationary" in name only. They generally contain a propulsion system, and are frequently moved about in their assigned "box" of space, to prevent them from colliding with neighboring satellites. Sometimes they are moved from one assigned location to a different location, which could be on the other side of the Earth (as happened to AMC-4). When they have reached the end of their useful lives, they are re-orbited into a non-"stationary" "graveyard" orbit. The consequence of these movements is that identification of the various geo satellites via standard techniques may result in mis-identification ("cross tagging") due to the various motions of the satellites. It would be desirable to be able to tell them apart via electro-optical signatures unique to the individual satellites.

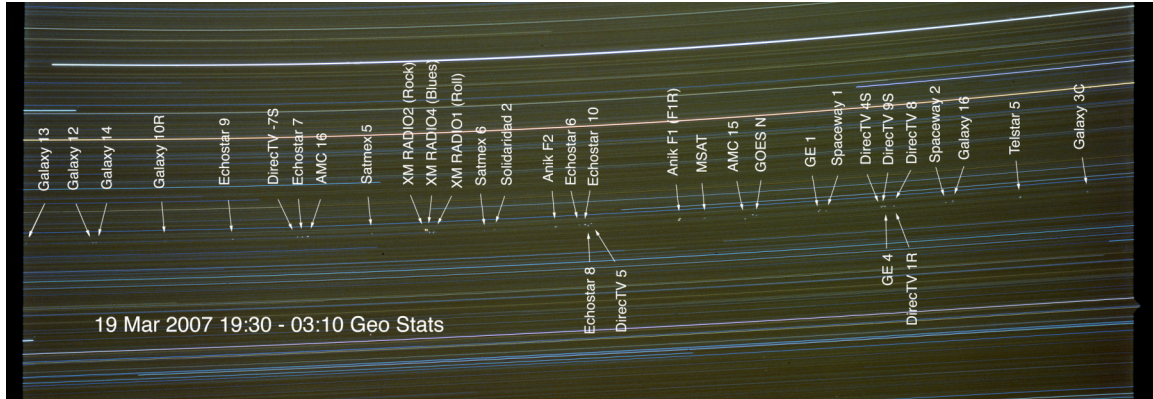


Fig. 1. Geostationary satellites [1]. Taken from Arizona, this photograph shows the geo satellite belt. The view from Maui is similar (but not identical). Several of the satellites seen in this image have been observed by us and are part of this paper.

As can be seen in Fig. 1, with imaging we can detect the light coming from the geo satellites, and can measure their location on the plane of the sky. However, given the current state-of-the art available at most observatories, resolving details on the satellites (e.g. their solar panels) is generally not possible; they are too faint and far away. For a telescope on Earth with $\sim 1/2$ arc-second angular resolution, the resolution element at the distance of the geo belt is ~ 80 meters; larger than the satellites themselves! Efforts are underway to improve this situation using adaptive optics [2], but these techniques are still limited by the distance and faintness of the targets.

We have investigated the application of spectrophotometric techniques to the geo satellite “cross tagging” problem. Spectrophotometry is the accurate measurement of the flux of light coming from a space object, the flux being resolved by the wavelength of each photon of light. Spectrophotometry is distinguished from color photometry in that color photometry makes sequential measurements of the flux of light through broad bandpass color filters [3], while spectrophotometry generally makes simultaneous measurements in all wavelengths available to the detector, and the measurement of the wavelengths of the incoming photons is orders of magnitude finer. Our goal has been to determine observable signatures that will allow for the identification of resident space objects.

2. OBSERVATIONS

Our initial observations of geo satellites were reported previously [4]. Those results included only a few spectra taken on three geo satellites, but were important as they demonstrated our ability to collect spectrophotometric data on faint geo satellite targets with this sensor. Since then, we have had several observational campaigns during the last 1.5 years, and have successfully collected data on over ten different geo satellites, often times on different campaigns, with a goal of collecting spectra at different phase angle values for each satellite. Table 1 lists the geo satellites we have observed. In addition to the geo satellites reported here, some observations of various low Earth orbit objects have been carried out, but will not be covered here.

Table 1 lists the names of geo satellites observed, and the observing run when the observations were made. The number of x's indicates the number of nights during a run that data were collected on that satellite.

Satellite	July 2006	August 2006	October 2006	January/February 2007	April/May 2007
AMC-4				xxx	
AMC10	x				
AMCS1				x	
ANIKF1					xx
ANIKF1-R					xx
DirecTV-1R				xx	
DirecTV2				x	
DirecTV5		x			
Echostar		x			
Galaxy12					x
Goes10		xx			
Intelsat510		x		x	
Orion 3		x			
TDRS5		x			xxx
TDRS7	x	x	x	xxxx	xxx
TDRS8			x	xxxx	
XM1					x
XM2					xx

Most of the observations have been made with the BASS sensor, in the 3-13 micron bandpass, but we also have collected a small amount of data with two different near-IR spectrographs, namely the Hi-VIS at AEOS, and the SPEX at the IRTF.

As part of the geo satellite observations, it is a requirement on our part to collect spectra on IR standard calibration stars (see Table 2). This allows recovery of absolute radiometric measurements. A nightly observing campaign consists of a mix of satellites and calibration stars [5], ordered to allow calibration star data that is collected at a similar air mass to the geo satellite, as well as at a similar location in the sky, and nearby in time to the satellite data. This is necessary to assure that the atmospheric conditions for the viewing paths for both the target satellite and the calibration star are as similar as can be obtained.

Table 2 lists the five IR calibration stars utilized by BASS to obtain absolutely calibrated spectra of targets. The five are all relatively bright and stable in their infrared emission. Vega (α Lyr) defines the 0th magnitude point. About 30 years of data show these five to be constant in flux relative to each other at the 1% level.

Calibrator type	Designation	Historic Name
Primary	α Lyr	Vega
Secondary	α Tau	Aldebaran
Secondary	β Gem	Pollux
Secondary	α CMa	Sirius
Secondary	α Boo	Arcturus

3. SENSORS

BASS

The BASS instrument has been described elsewhere in detail [6,7]. Briefly, it utilizes NaCl and CaF₂ crystals to disperse 3-13.5 micron light onto linear arrays of Si BIBIB detectors, sampled at ~200 Hz. It is liquid helium cooled (detectors and internal optics), has a field of view of ~4.7 arcseconds, and incorporates a Princeton CCD camera and filter wheel for real-time guiding. We have constructed a custom optics bench on the AEOS telescope to accommodate BASS. Fig. 2 shows the details of the internal optical layout, and Fig. 3 shows the BASS mounted on the AEOS telescope.

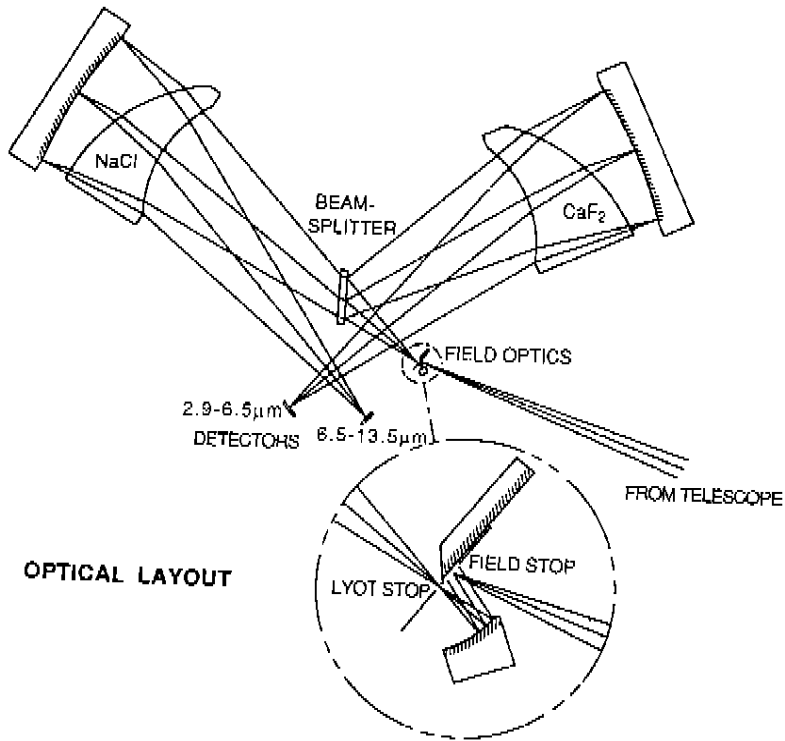


Fig. 2. Dual-curved crystals resolve and focus light onto array of silicon BIBIB detectors [6]. Single aperture covers 3-13.5 micron range. Detectors and internal optics contained inside dewar housing and cooled to liquid helium temperatures.

The AEOS telescope at AMOS is very suitable for observing with BASS, as it has both a chopping secondary, as well as the ability to “nod” the telescope on- and off-source. The chopping secondary provides an on-source “A” position, and an off-source “B” position, while the nodding of the telescope shifts the target to the “B” position, and also provides a new off-source position. This somewhat complicated observing arrangement allows us to measure (and then subtract) both sky and telescope backgrounds, which would otherwise dominate our measurements. The “throw” and the frequency of the chopping and nodding is adjustable, and is all under control of the BASS data collection workstation.



Fig. 3. Two photographs showing BASS's accommodation on the AEOS telescope. The left-hand photo shows the BASS enclosure (right), conjoined with the long wavelength IR imager (left), with the 3.6 m primary mirror behind and to the right. The right-hand image shows the BASS dewar mounted inside the enclosure (cover removed for clarity). Below the sliding shelf that BASS rests on is mounted the CCD camera that is used for real-time telescope guiding on targets.

Hi-VIS

The Hi-VIS spectrograph is a cross-dispersed Echelle spectrograph that is a facility instrument at AEOS. It has both visible and near-IR (1-2.5 micron) cryogenically cooled detector systems, but for these observations we only utilized the near-IR arm of Hi-VIS. Fig. 4 shows the Hi-VIS optical layout and characteristics of the IR channel. The instrument has previously been described in more detail [8, and references therein].

Table 3 describes some of the aspects of the Hi-VIS near-IR spectrograph channel.

Near-IR Channel Characteristics				
• Wavelength range:	1.0 – 2.5 μm	(3 cross gratings)		
• Image Scale:	0.16 arcsec / pixel			
• Science Camera:	18 μm pixel	2Kx2K HgCdTe hybrid		
• Slit-image Camera:	512x512 HgCdTe, 0.12" / pixel			
• J,H,K pre-filters				
• Resolution (theoretical):	60,000 (0.23" slit, bin1)			

Grating	Ruling	Blaze Angle	Order	Echelle Orders
J	400 l/mm	15.0°	1	42-51
H	300 l/mm	14.8°	1	31-39
K	200 l/mm	15.0°	1	24-30

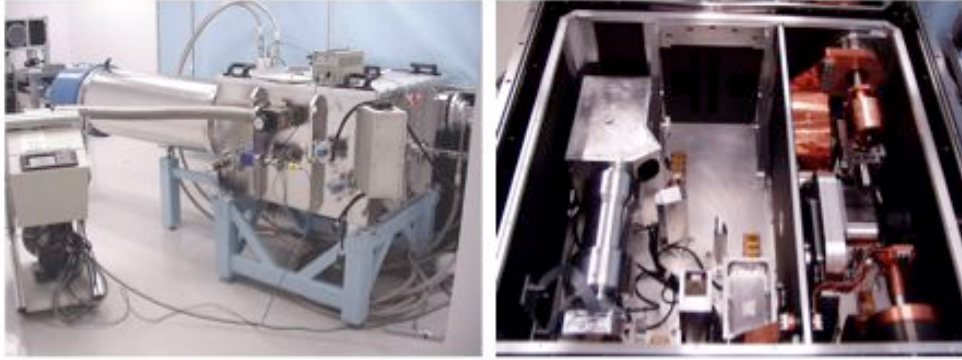


Fig. 4. Photographs of the Hi-VIS spectrograph near-IR channel. The satellite data described here were taken with this instrument at AEOS, on two nights, using the H & K band gratings. On the first night, data were collected on a set of geo satellites by Hi-VIS, followed that night with BASS collecting data on the same set of satellites. The following night the roles were reversed; BASS collected first on the same set, then Hi-VIS. This was to allow better phase angle coverage by the two instruments.

SpeX

In addition to the near-IR spectra collected with Hi-VIS, we have also collected some sample spectra on TDRS7 using NASA’s Infrared Telescope Facility (IRTF) SpeX 0.8-5.4 micron spectrograph [9], located on Mauna Kea. Although SpeX has lower resolution (~1000 v. 60,000 for Hi-VIS), it collects data that overlap with the BASS band pass (NB: the sample data we collected on TDRS7 with SpeX is in the 0.8-5.4 micron range), and it can also collect spectra with a desired signal-to-noise ratio in much less time than the Hi-VIS can.

4. DATA ANALYSIS

The BASS geo satellite analysis relies heavily on previous and on-going work [5] to monitor spectrophotometric standard stars in support of a satellite program. The data analysis tools and methods utilized for the secondary calibrators are directly applicable to the analysis of data collected on the geo satellites. The secondary calibrator monitoring program has some very stringent accuracy requirements (10% accuracy, with a goal of 8%; we seem to achieve 4-5% on many of the secondary calibrators [10]). One of the guiding principles followed to achieve this is to measure what we can, as accurately as we can, to avoid having to model complicated elements such as the atmosphere. Hence the previously described rather complicated chopping and nodding regimens adhered to while taking data. But this also follows into the analysis of the data collected.

The basic “unit” of data collected is a “nod pair”, which is the weighted, background-subtracted signal with on- and off-source data. There are typically 6-26 nod pairs in a data file, and usually 3-5 data files are taken on an object at one time. As part of the data analysis process, all pairs are quality checked (e.g., for instrument glitches or guiding problems, etc.) and accepted or rejected from further analysis. Accepted pairs are combined and corrected for detector non-linearities. The intermediate result is the signal strength of the target (in say, volts) as a function of wavelength. See Fig. 5 for an example of some of the steps followed. This process is repeated for a calibration star observed at a similar air mass, and then the target spectrum is divided by the (air mass corrected) calibration star spectrum. Atmospheric corrections may be applied at this point if needed; typically we exclude from further analysis parts of the spectrum for which the atmosphere is opaque. There are only a few IR primary calibration standard stars, as they need to be bright, well-characterized, stable, and have accurate flux models. The flux model for the observed calibration star is multiplied by the ratio of the target spectrum divided by the measured calibration star spectrum, which allows the calculation of the spectrum of the target with absolute radiometric flux units (e.g., $W/cm^2/micron$).

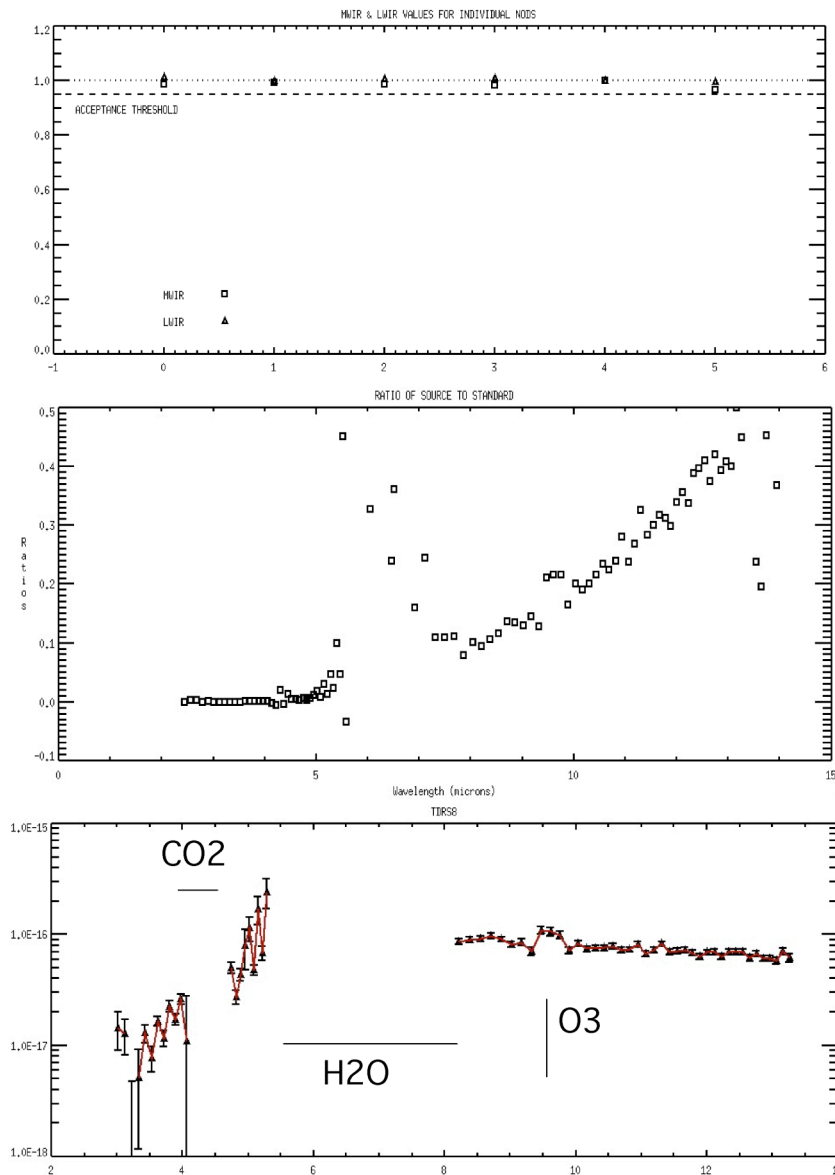


Fig. 5 illustrates some of the steps in the data analysis process. Nod pairs (weighted, back-ground subtracted signal) are compared against thresholds as a quality check and accepted or rejected (top graph). The nod pairs of the target object are combined and corrected for detector non-linearities; this process is repeated for the calibration star measurements, the two spectra are corrected for differences in air mass, and the target is divided by the calibration star (middle graph). Radiometric flux units are recovered by multiplication of this ratio by an accurate calibration star flux model (bottom panel). Major atmospheric absorption/emission bands are indicated as well.

Fig. 6 shows three different spectra from geo satellites. What can be seen is a fairly smooth spectrum, Plankian in shape, and lacking any strong emission or absorption features (other than residual atmospheric features).

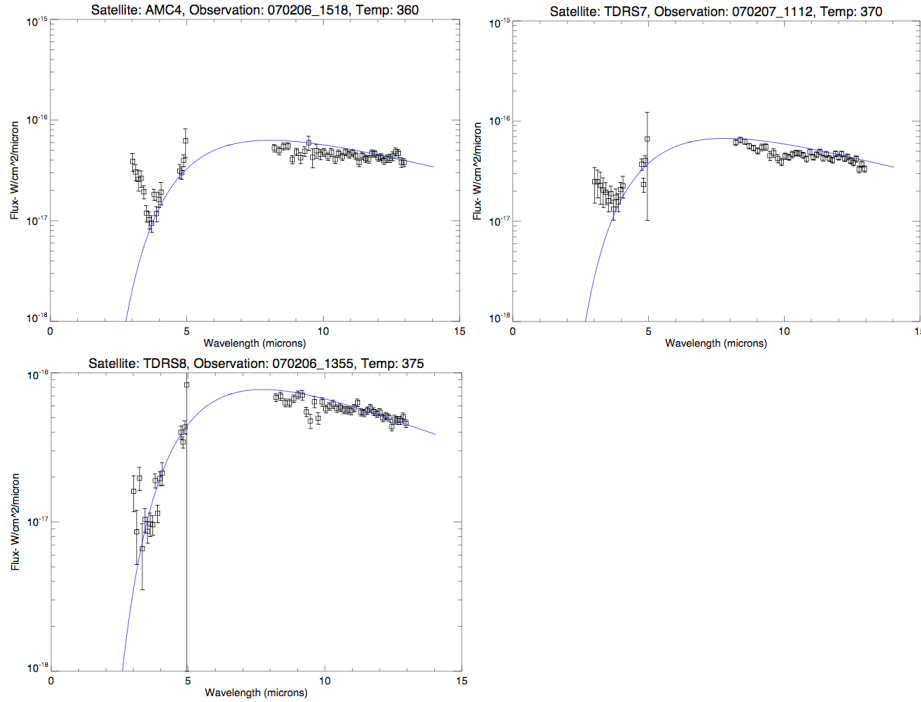


Fig. 6. BASS spectra of geo satellites AMC-4, TDRS7, and TDRS8. The data were processed in the fashion described above. Here we have fitted Planck functions to the thermal part of the spectra, and derived a color temperature (described below in the text). Other than incompletely removed atmospheric features (and artifact of residual atmospheric differences between the target and the calibration star), we see no strong evidence of absorption or emission features from the satellites.

Building on previous work [11], we have made repeated observations of several satellites at differing phase angles. The phase angle is defined in this case as the angle between the ray from the satellite to the Sun, and the ray from the satellite to the observer. Given we generally only make nighttime observations of geo satellites, full phase angular coverage is not available to us, and what range of phase angle is available depends on the location of a given satellite. See Fig. 7 for examples of available phase angles.

Fig. 8 shows the dependency of the spectrum on the phase angle for a typical geo satellite. We find that the thermal emission (which can be characterized by the 8-13 micron flux) varies to a much greater extent than does the reflected solar emission (the flux below 4 microns). If we plot just the thermal emission as a function of phase angle, Fig. 9, what we find is a general trend of minimum flux at phase angles ~ 90 degrees, with thermal flux increasing with larger or smaller phase angles. However, while this general trend holds, in at least one example there would appear to be a distinct signature difference in the flux v. phase angle curves for two geo satellite; in this case AMC-4 and DIRECTV-1R. It is interesting to note that although these two satellites are very close together in space, and have the same range of phase angles available to us, their dependency of flux with phase angle is distinctly different.

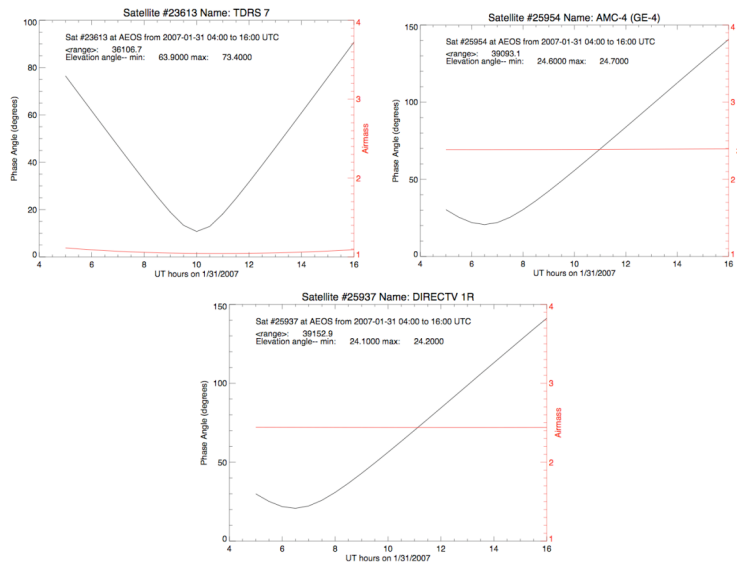


Fig. 7 shows the calculated phase angles for the night of January 31 2007 for three geo satellites (TDRS7 (top left), AMC-4 (top right) and DirecTV-1R (bottom panel), as observed from AEOS on Maui. AMC-4 and DirecTV-1R are adjacent in the geo belt, and hence their almost identical phase angle curves. Due to geographical and sun-angle constraints, not all possible phase angles (0-180 degrees) are available to observers.

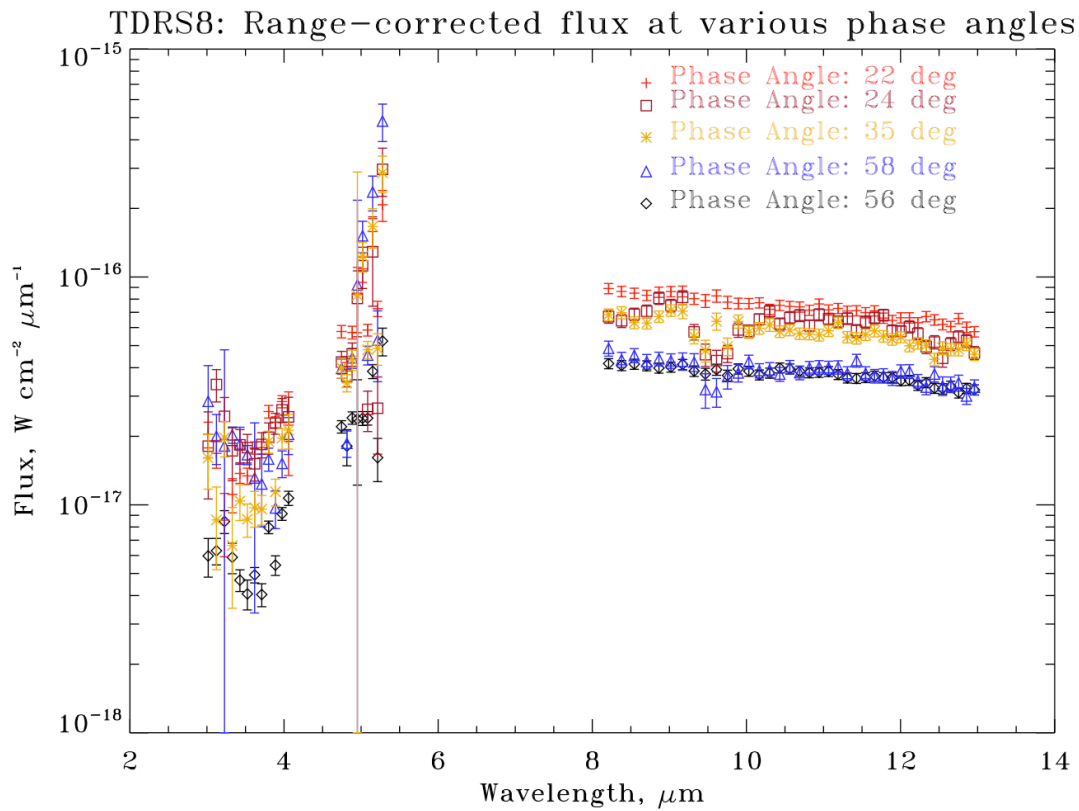


Fig. 8 shows the 3-13 micron spectra collected on TDRS8 at 5 different phase angles (22°-58°). The thermal part of the spectrum (8-13 microns) shows a strong dependency on phase angle. Also, each phase angle was collected on a different night (some in October 2006, the remainder in January & February of 2007). The thermal spectra appear to be stable over at least several months.

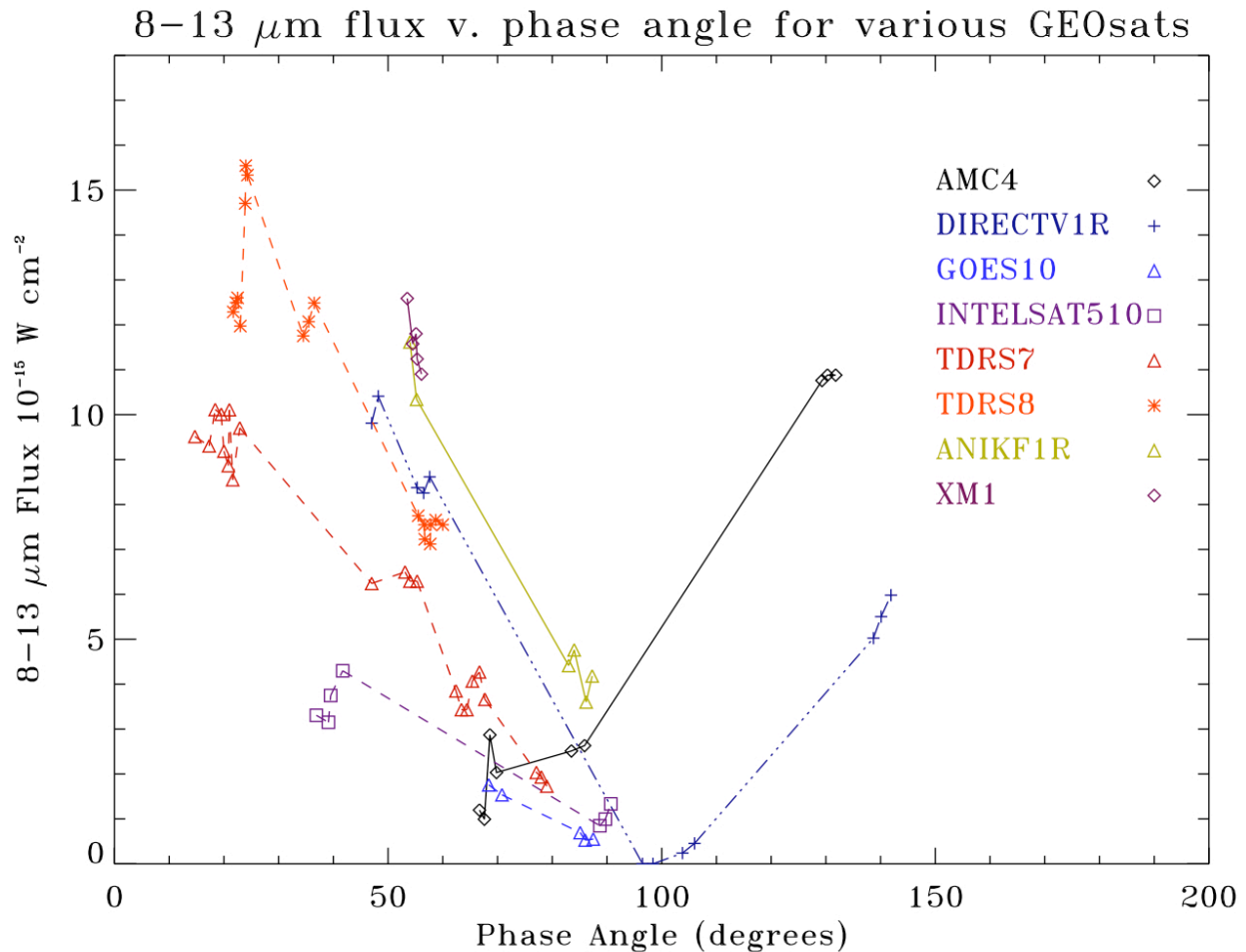


Fig. 9 shows the integrated thermal 8-13 micron flux for several geo satellites as a function of phase angle. Generally the trend is a “V” shape with the minima at $\sim 90^\circ$ phase angle. However, note the distinct signature differences between AMC-4 and DirecTV-1R, which are adjacent in the geo belt.

Unlike for some low Earth orbiting satellites, the size and range of a geo satellite creates an angular subtense smaller than the angular resolution of most currently available optical systems; this impacts both imaging and spectroscopic observations. As we cannot spatially resolve the geo satellite, the light that we detect from the satellite is a mixture of emission (reflected or thermal) from the various parts of the satellite; e.g., the solar panels, the spacecraft body, the antennas and transmitters, etc. Thus, the spectra we observe from these non-resolved objects are a blend of the various emissions from the various parts of the object. For the thermal part of the spectra, we can fit a Planck function to the spectra, which has only two free parameters: the flux level (which depends on the area, the emissivity of emitting surface, and the range to the target), and the “temperature” of the target (which determines the “shape” of the Planck function). Since the flux is from various parts of the satellite, and presumably the temperature of individual parts of satellite varies, the temperature we associate with this blended thermal flux is referred to by Astronomers as the “color temperature”.

We have taken our various spectra for different geo satellites at different phase angles and fit Planck functions to them, adjusting the flux level and color temperature to minimize differences from the model to the observed thermal data points. Some representative fits are shown in Fig. 6. Generally, the data can be represented by a single Planck function at a given temperature and flux level, but in some instances the “single Planck function” model breaks down, and does not fit the data well.

Plotting the fit-derived color temperatures for various geo satellites as a function of phase angle yields some interesting patterns, as may be seen in Fig. 10. While still data-limited, what we are seeing in some instances is behavior that mirrors the flux-vs.-phase angle curves; a “V” shape, albeit inverted with respect to the curves in Fig. 9, although with much greater individuality.

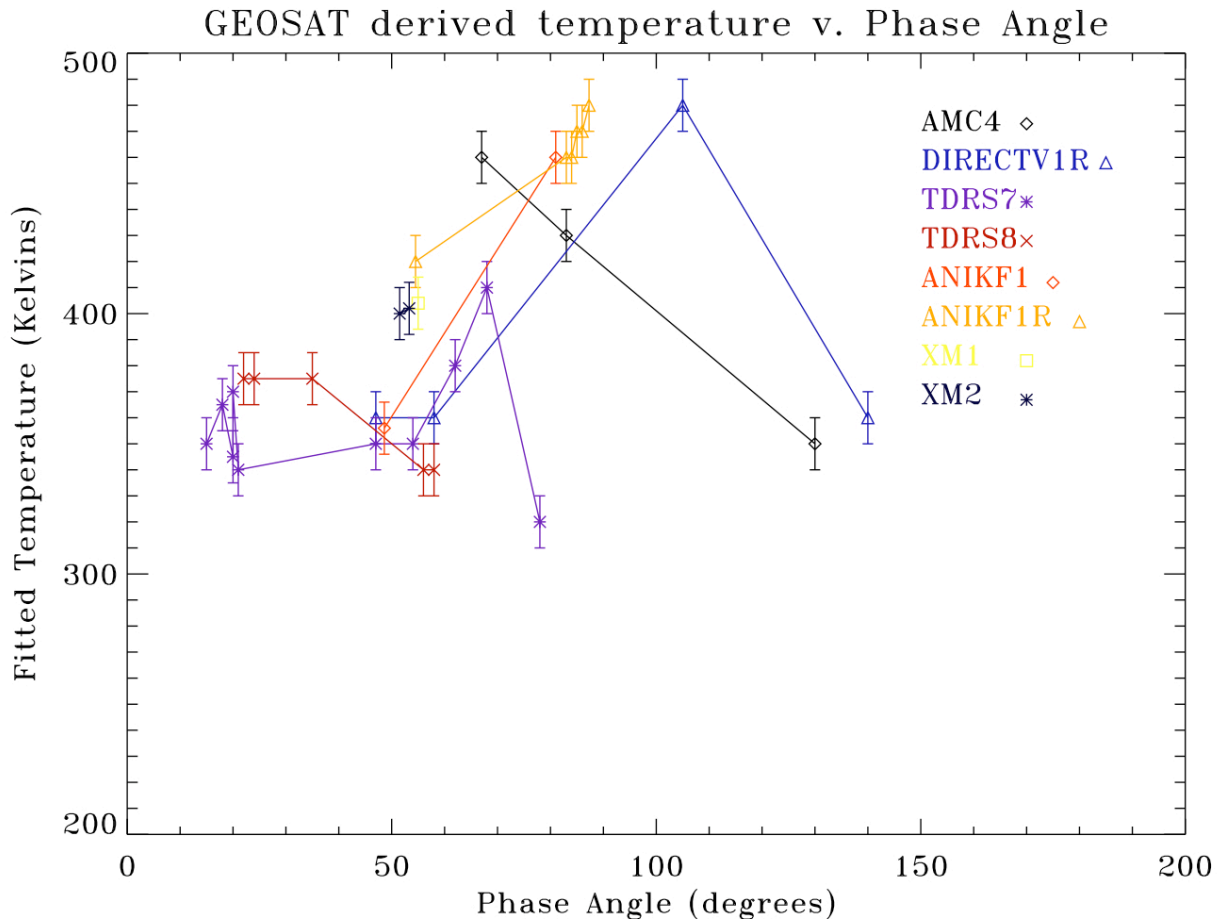


Fig. 10. Fitting Planck functions to geo satellite spectra yields a color temperature estimate for those spectra; for various satellites at various phase angles we plot the color temperature estimate. In general, color temperature changes with phase angle, and in some cases the lower (higher) flux spectra are fit with a higher (lower) temperature. We find greater differences between the temperature v. phase angle curves compared to the flux v. phase angle curves.

At first glance it seemed counter-intuitive that the color temperatures derived from phase angles with the lower flux levels would be the hottest. We can assume a fairly simple and crude morphological model for a geo satellite, consisting of:

- a. Solar panels, large and with a high surface area to thickness ratio, which are (generally) maintained pointed at the Sun
- b. A spacecraft bus; a cube wrapped in thermal blankets to keep the avionics at near room temperature
- c. An Earth-facing transmitter (or transmitters), which for a telecommunications satellite would have a fairly high duty-cycle.

This fairly crude satellite model does help us to understand some of the trends we see in the data. For small (large) phase angles we are seeing the front (back) of the solar panels; given their large area, emission from the solar panels should dominate when observed at large or small phase angles. When observing at phase angles of ~90 degrees, we are seeing the (Sun-pointed) solar panels nearly edge-on. Thus, this would seemingly explain the flux minima observed around phase angles of ~90 degrees, with flux increasing as we go to smaller or larger phase angles.

When looking at phase angles ~ 90 degrees, the flux from the satellite is no longer dominated by the flux from the solar panels, and in some instances seems to correspond to a larger color temperature. Unlike an asteroid or meteor, an active satellite has various subsystems that change the overall thermal balance of the object to more than just “absorb and emit”. A satellite’s solar panels convert sunlight into electricity, which is stored in on-board batteries. Heaters and radiators maintain some parts of the satellite within narrow temperature ranges. Also, energy is withdrawn from the solar panels and batteries and used to power the transmitters (e.g., dish antennas sending down television signals). One hypothesis is that when we are observing some satellites at ~ 90 degrees phase angle; we are seeing mostly the flux from (hot) transmitters (and possibly the cooler spacecraft bus ‘behind’ the transmitters). More analysis needs to be done to ascertain the source of these apparent temperature changes, such as calculating the emissivity-area as a function of phase angle.

During the 2007 January/February observing run, we collected data on three geo satellites, on two nights, using both BASS and the HiVIS spectrograph. HiVIS data were collected using both the H and the K gratings. As the time required to change over from one instrument to the other is somewhat lengthy, we utilized the following scheme to good phase angle coverage of the satellites while maximizing observing time: on the first night, the HiVIS observed the three satellites first, in both H and K, followed by BASS observing all three satellites. The second night, we observed the satellites first with BASS, then with the HiVIS. Both sensors also observed the necessary calibration stars to determine absolutely calibrated radiometric flux. An example of combined spectra for one satellite, AMC-4, can be seen in Fig. 11.

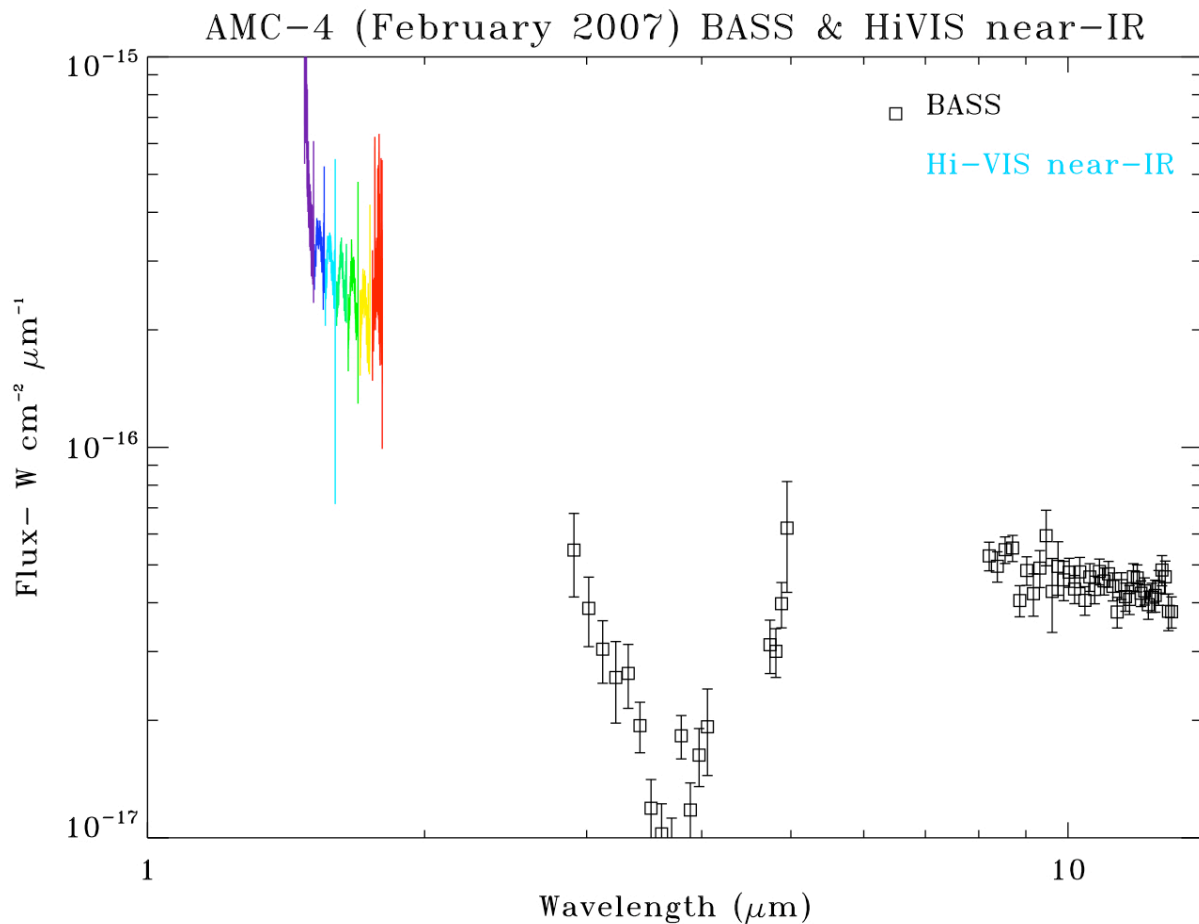


Fig. 11. Combined HiVIS (<2 micron (H-band grating)) and BASS (3-13 micron) spectra of AMC-4.

In addition to the HiVIS data collections, we have also collected a limited amount of data on the IRTF SpeX instrument on TDRS7, in the 0.8-2.4 micron range. Fig. 12 shows these data plotted along with BASS data on the same satellite (but not taken at the same time).

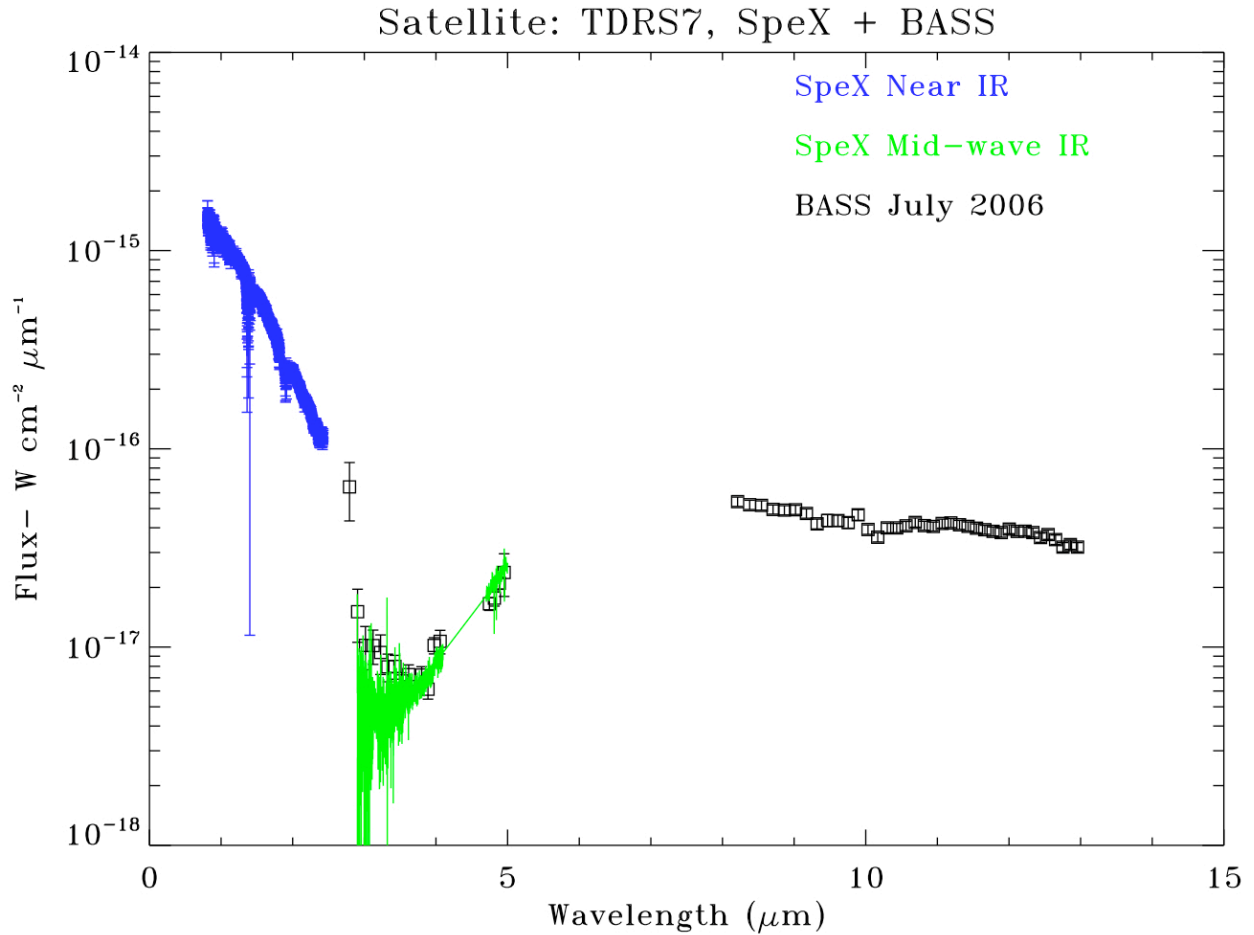


Fig. 12. SpeX data (0.8-2.4 micron) are plotted along with BASS data (3-13 microns). The SpeX data were collected in July of 2007 (at the IRTF), the BASS data in July of 2006 (at AEOS). As was the case in Fig. 11 with the HiVIS data, the two independent absolute flux measurements “line up” well.

5. DISCUSSION

We have collected multiple spectra on a set of geo satellites, on different dates, and at different solar phase angles. The data collected are repeatable, given the same set of observing conditions. We find that the spectra can be described roughly as featureless black bodies. Other than possible atmospheric features, we see no evidence of emission or absorption spectral features. We find that the satellite thermal emission detected varies with the solar phase angle, and can be understood in terms of a crude model of a geo satellite. We find that in general we can estimate a color temperature for the satellites based upon Planck function fits to the thermal spectra. We find variability of the dependence for color temperature fits on solar phase angle that in some cases may also be explained by a crude geo satellite model, and that may be used as an observable “fingerprint” to distinguish between near-by geo satellites. We plan to collect more data on geo satellites, as well as to increase the fidelity of the geo satellite thermal model we are testing against our data.

6. REFERENCES

1. Photograph was taken on Kitt Peak in Arizona (lat=31.95°, long=248.5°), 20 Mar 2007, 2:30-11:00 UT. Camera was fixed and spanned 232.5° to 266.5° east longitude along the celestial equator. Setting was f/6.3; focal length=80 mm; film: Ektachrome 100 G. Photo by Bill Livingston, National Solar Observatory.
2. Worden, Simon P., Lloyd-Hart, Michael, Hinz, Phil, Hege, Keith, McCarthy, Don, Angel, Roger, Miller, Doug, Kenworthy, Matthew, Jefferies, Stuart M., Hope, Douglas. "Observing Deep Space Microsatellites with the MMT and Large Binocular Telescope", *2005 AMOS Technical Conference*, September 2005, Maui HI.
3. Payne, Tamara E., Gregory, Stephan A., Luu, Kim. "SSA Analysis of GEOS Photometric Signature Classifications and Solar Panel Offsets", *2006 AMOS Technical Conference*, September 2006, Maui HI.
4. Lynch, David K., Russell, Ray W., Gutierrez, David, Turpin, Mark, Crawford, Kirk, Dotan, Yaniv, Kim, Daryl, Rudy, Richard J., Skinner, Mark A. "3-13 micron Spectra of Geosynchronous Satellites", *2006 AMOS Technical Conference*, September 2006, Maui HI.
5. Lynch, D. K., et al., "Infrared Stellar Calibration and AMOS", *2004 AMOS Technical Conference*, September 2004, Maui, HI, A1-28.
6. Hackwell, J.A., et al., "A low resolution array spectrograph for the 2.9 to 13.5 micron spectral region", *Proc SPIE 1235* (1990), 171.
7. Russell, R., et al., "New Thermal IR Spectroscopic Capability on AEOS", *2005 AMOS Technical Conference*, September 2005, Maui, HI, 279-286.
8. Whitman, Kathryn, Harrington, David M., Kuhn, Jeffrey R., "The HiVIS Spectrograph at AEOS: A Unique Tool for Visible and Infrared Spectroscopy", *AMOS Technical Conference*, September 2005, Maui, HI, 270-278.
9. Rayner, J. T., Toomey, D. W., Onaka, P. M., Denault, A. J., Stahlberger, W. E., Vacca, W. D., Cushing, M. C., and Wang, S. "SpeX: A Medium-Resolution 0.8-5.5 micron Spectrograph and Imager for the NASA Infrared Telescope Facility" (2003, PASP 115, 362).
10. Ray W. Russell, private communication.
11. Payne, Tamara E.; Gregory, Stephen A.; Houtkooper, Nina M.; Burdullis, Todd W., *Astronomical Data Analysis II*. Edited by Starck, Jean-Luc; Murtagh, Fionn D. *Proceedings of the SPIE*, Volume 4847, pp. 332-336 (2002).